Catalytic Effects of Dioxygen on Intramolecular Electron Transfer in Radical Ion Pairs of Zinc Porphyrin-Linked Fullerenes

Shunichi Fukuzumi,*,§ Hiroshi Imahori,*,§ Hiroko Yamada,§ Mohamed E. El-Khouly,† Mamoru Fujitsuka,† Osamu Ito,*,† and Dirk M. Guldi*,‡

Contribution from the Department of Material and Life Science, Graduate School of Engineering, Osaka University, CREST, Japan Science and Technology Corporation, Suita, Osaka 565-0871, Japan, Institute for Chemical Reaction Science, Tohoku University, Sendai, Miyagi 980-8577, Japan, and Radiation Laboratory, University of Notre Dame, Notre Dame, Indiana 46556

Received June 9, 2000. Revised Manuscript Received December 28, 2000

Abstract: Dioxygen accelerates back electron transfer (BET) processes between a fullerene radical anion (C_{60}) and a radical cation of zinc porphyrin (ZnP) in photolytically generated **ZnP**$^{\bullet+}$**-C$_{60}$**$^{\bullet-}$ and **ZnP**$^{\bullet+}$**-H$_2$P-C$_{60}$**$^{\bullet-}$ radical ion pairs. The rate constant of BET increases linearly with increasing oxygen concentration without, however, forming reactive oxygen species, such as singlet oxygen or superoxide anion. When ferrocene (Fc) is used as a terminal electron donor moiety instead of ZnP (i.e., **Fc-ZnP-C$_{60}$**), no catalytic effects of dioxygen were, however, observed for the BET in **Fc**$^{+}$**-ZnP-C$_{60}$**$^{\bullet-}$, that is, from $C_{60}^{\bullet-}$ to the ferricenium ion. In the case of ZnP-containing C_{60} systems, the partial coordination of O_2 to ZnP$^{\bullet+}$ facilitates an intermolecular electron transfer (ET) from $C_{60}^{\bullet-}$ to O_2. This rate-determining ET step is followed by a rapid intramolecular ET from $O_2^{\bullet-}$ to ZnP$^{\bullet+}$ in the corresponding $O_2^{\bullet-}$-ZnP$^{\bullet+}$ complex and hereby regenerating O_2. In summary, O_2 acts as a novel catalyst in accelerating the BET of the $C_{60}^{\bullet-}$-ZnP$^{\bullet+}$ radical ion pairs.

Introduction

Widespread efforts have been directed to achieve long-lived charge-separated states in artificial photosynthesis by varying one or more of the following parameters: (i) the redox properties of the donor and acceptor moieties, (ii) the distance of the donor−acceptor pair, and (iii) the reorganization energy of, for example, the electron acceptor.[1−4] These studies demonstrated that the electron transfer (ET) rates are determined in large by a combination of these factors. Thus, once an adequate donor−acceptor pair is fixed via any of these parameters, attenuation of the underlying rate is rendered rather difficult. However, a number of recent examples report on photoinduced ET reactions, which reveal a significant acceleration in the presence of a third component acting as a catalyst.[5,6] Most importantly, photochemical redox reactions, which would otherwise be unlikely to occur, proceed efficiently via the selective catalysis of the individual ET steps.[5,6] Up to this end, effective catalysts for accelerating ET reactions have so far been limited to acids or metal ions which interact with the generated products.[5,6]

We wish to present herein that a simple molecule, such as dioxygen, can be employed as a powerful catalyst in accelerating the back electron transfer (BET) from a fullerene radical anion to a zinc porphyrin radical cation within photolytically generated radical ion pairs. This is the first example in which O_2, the most important biological oxidant, acts as a catalyst rather than an oxidant in BET reactions. The effects of O_2 were compared in different types of porphyrin-containing C_{60} linked systems shown in Figure 1 to elucidate the catalytic mechanism in which oxygen participates in mediating BET reactions.

Experimental Section

Materials. The synthesis and characterization of the porphyrin−fullerene linked molecules and reference compounds (**ZnP-C$_{60}$**,[7,8] **ZnP-H$_2$P-C$_{60}$**,[8] **Fc-ZnP-C$_{60}$**,[9] and **C$_{60}$-ref**[10]) have been described previously (see Figure 1). Tetrabutylammonium hexafluorophosphate used as a supporting electrolyte for the electrochemical measurements was obtained from Tokyo Kasei Organic Chemicals. Benzonitrile was

* To whom correspondence should be addressed. E-mail: fukuzumi@ap.chem.eng.osaka-u.ac.jp; imahori@ap.chem.eng.osaka-u.ac.jp; guldi.1@nd.edu; ito@icrs.tohoku.ac.jp.

§ Osaka University.

† Tohoku University.

‡ University of Notre Dame.

(1) (a) Page, C. C.; Moser, C. C.; Chen, X.; Dutton, P. L. *Nature* **1999**, *402*, 47. (b) Gust, D.; Moore, T. A. In *The Porphyrin Handbook*; Kadish, K. M., Smith, K. M., Guilard, R., Eds.; Academic: San Diego, CA, 2000; Vol. 8, pp 153−190. (c) Langen, R.; Chang, I.-J.; Germanas, J. P.; Richards, J. H.; Winkler, J. R.; Gray, H. B. *Science* **1995**, *268*, 1733. (d) Winkler, J. R.; Gray, H. B. *Chem. Rev.* **1992**, *92*, 369.

(2) (a) Wasielewski, M. R. In *Photoinduced Electron Transfer*; Fox, M. A., Chanon, M., Eds.; Elsevier: Amsterdam, 1988; Part A, p 161. (b) Wasielewski, M. R. *Chem. Rev.* **1992**, *92*, 435. (c) Jordan, K. D.; Paddon-Row, M. N. *Chem. Rev.* **1992**, *92*, 395.

(3) (a) Verhoeven, J. W. *Pure Appl. Chem.* **1990**, *62*, 1585. (b) Verhoeven, J. W.; Scherer, T.; Willemse, R. J. *Pure Appl. Chem.* **1993**, *65*, 1717.

(4) (a) Imahori, H.; Y. Sakata, Y. *Adv. Mater.* **1997**, *9*, 537. (b) Fukuzumi, S.; Imahori, H. In *Electron Transfer in Chemistry*; Balzani, V., Ed.; Wiley-VCH: Weinheim, 2001; Vol. 2, in press. (c) Guldi, D. M. *Chem. Commun.* **2000**, 321. (d) Imahori, H.; Sakata, Y. *Eur. J. Org. Chem.* **1999**, 2445.

(5) Fukuzumi, S.; Itoh, S. In *Advances in Photochemistry*; Neckers, D. C., Volman, D. H., von Bünau, G., Eds.; Wiley: New York, 1998; Vol. 25, pp 107−172.

(6) Fukuzumi, S. In *Electron Transfer in Chemistry*; Balzani, V., Ed.; Wiley-VCH: Weinheim, 2001; Vol. 5, in press.

(7) Yamada, K.; Imahori, H.; Nishimura, Y.; Yamazaki, I.; Sakata, Y. *Chem. Lett.* **1999**, 895.

(8) (a) Tamaki, K.; Imahori, H.; Nishimura, Y.; Yamazaki, I.; Sakata, Y. *Chem. Commun.* **1999**, 625. (b) Luo, C.; Guldi, D. M.; Imahori, H.; Tamaki, K.; Sakata, Y. *J. Am. Chem. Soc.* **2000**, *122*, 6535.

(9) Fujitsuka, M.; Ito, O.; Imahori, H.; Yamada, K.; Yamada, H.; Sakata, Y. *Chem. Lett.* **1999**, 721.

(10) Imahori, H.; Ozawa, S.; Ushida, K.; Takahashi, M.; Azuma, T.; Ajavakom, A.; Akiyama, T.; Hasegawa, M.; Taniguchi, S.; Okada, T.; Sakata, Y. *Bull. Chem. Soc. Jpn.* **1999**, *72*, 485.

10.1021/ja002052u CCC: $20.00
Published on Web 02/22/2001

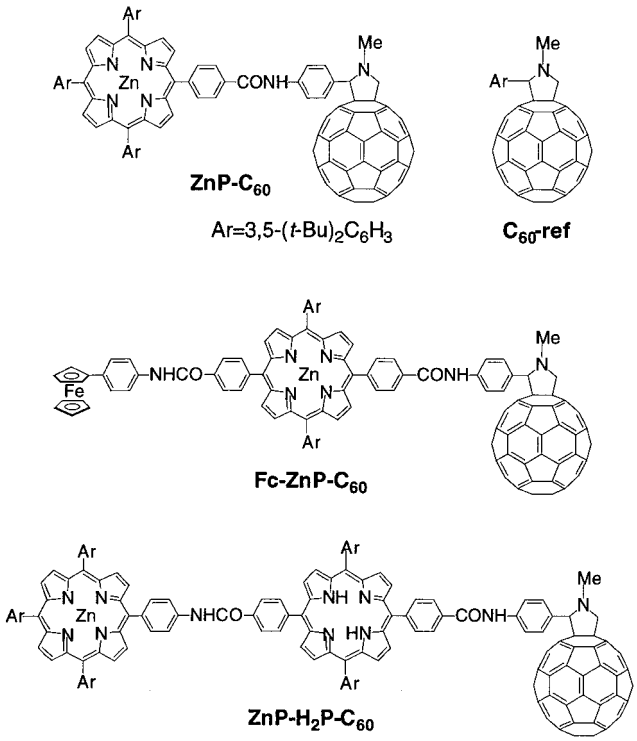

Figure 1. Structures of molecular dyad, triads, and reference used in this study.

purchased from Wako Pure Chemical Ind., Ltd., and purified by successive distillation over calcium hydride. 1,1-Dihexyl-4,4′-dipyridinium dibromide and the corresponding diperchlorate salt were prepared according to the following procedure.[11]

1,1-Dihexyl-4,4′-dipyridinium dibromide: 4,4′-Dipyridine (2.5 g, 16 mmol) and 1-bromohexane (11.5 g, 70 mmol) were dissolved in 15.6 mL of DMF. The mixture was heated to reflux for 3 h. After cooling, the yellow precipitate was filtered and rinsed with ethanol. The precipitate was recrystallized from CH_3CN and 4.7 g of a light yellow solid was obtained. Yield 60%. Mp 259−261 °C dec. Melting points were recorded on a Yanagimoto micro-melting apparatus and are not corrected. ^{1}H NMR spectra were measured on a JEOL EX-270. Fast atom bombardment mass spectra were measured on a JEOL JMS-DX303HF. ^{1}H NMR (270 MHz, D_2O) δ 8.96 (d, $J = 6$ Hz, 4H), 8.39 (d, $J = 6$ Hz, 4H), 4.58 (t, $J = 7$ Hz, 4H), 1.94 (m, 4H), 1.20 (m, 12H), 0.71 (t, $J = 6$ Hz, 6H); MS(FAB) 488 ($M + H^+$). Calcd for $C_{22}H_{34}N_2Br_2$: C, 54.32; H, 7.04; N, 5.76. Found: C, 54.25; H, 6.86; N, 5.79.

1,1-Dihexyl-4,4′-dipyridinium diperchlorate (HV^{2+}): The obtained dibromide (2.0 g, 4.1 mmol) and sodium perchlorate (24.5 g, 0.2 mol) were dissolved in 100 mL of water and stirred for 20 h. The white precipitate was extracted with ethyl acetate and washed with water. The organic layer was dried over Na_2SO_4 and evaporated. The residue was rinsed with methanol and 1.1 g of a white solid was obtained. Yield 52%. Mp 279−281 °C dec. ^{1}H NMR (270 MHz, DMSO-d_6) δ 9.36 (d, $J = 6$ Hz, 4H), 8.75 (d, $J = 6$ Hz, 4H), 4.67 (t, $J = 7$ Hz, 4H), 1.96 (m, 4H), 1.30 (m, 12H), 0.87 (t, $J = 6$ Hz, 6H); MS(FAB) 524 ($M + H^+$). Calcd for $C_{22}H_{34}N_2O_8Cl_2$: C, 50.29; H, 6.52; N, 5.33. Found: C, 50.07; H, 6.33; N, 5.29.

Spectral Measurements. Nanosecond transient absorption measurements were carried out with SHG (532 nm) of a Nd:YAG laser (Spectra-Physics, Quanta-Ray GCR-130, fwhm 6 ns) as an excitation source. For transient absorption spectra in the near-IR region (600−1600 nm), monitoring light from a pulsed Xe-lamp was detected with a Ge-avalanche photodiode (Hamamatsu Photonics, B2834). Photoinduced events in micro- and millisecond time regions were estimated by using a continuous Xe-lamp (150 W) and an InGaAs-PIN photodiode (Hamamatsu Photonics, G5125-10) as a probe light and a detector, respectively. Details of the transient absorption measurements were described elsewhere.[8b] All the samples in a quartz cell (1 × 1 cm) were deaerated by bubbling argon through the solution for 15 min.

Near-IR luminescence emission spectra of singlet oxygen were measured on a Hamamatsu Photonics R5509-72 photomultiplier under irradiation at 462 nm with use of a Cosmo System LVU-200S monochromator.

Electrochemical Measurements. The cyclic voltammetry (CV) measurements were performed on a BAS 50W electrochemical analyzer in deaerated benzonitrile solution containing 0.10 M n-Bu_4NPF_6 as a supporting electrolyte at 298 K. The differential pulse voltammetry measurements were also performed on a BAS 50W electrochemical analyzer in a deaerated benzonitrile solution containing 0.10 M n-Bu_4NPF_6 as a supporting electrolyte at 298 K (10 mV s^{-1}). The glassy carbon working electrode was polished with a BAS polishing alumina suspension and rinsed with acetone before use. The counter electrode was a platinum wire. The measured potentials were recorded with respect to an Ag/AgCl (saturated KCl) reference electrode. Ferrocene/ferricenium was used as an external standard.

Results and Discussion

Time-resolved techniques, including fluorescence lifetime and transient absorption measurements, have been employed to probe the ET and BET dynamics in these donor−acceptor arrays, disclosing the crucial formation of $ZnP^{\bullet+}$-*spacer*-$C_{60}^{\bullet-}$ and Fc^+-*spacer*-$C_{60}^{\bullet-}$ pairs in a variety of solvents.[7−10,12] For example, a deoxygenated benzonitrile (PhCN) solution containing **ZnP-C$_{60}$** gives rise upon a 532 nm laser pulse to a characteristic absorption spectrum with maxima at 650 and 1000 nm (Figure 2a).[13] While the former maximum (i.e., 650 nm) is a clear attribute of the $ZnP^{\bullet+}$,[7−10,12] the latter maximum (i.e., 1000 nm) resembles the diagnostic marker of the fullerene radical anion.[7−10,12,14] The decay of both absorption bands obeys clear first-order kinetics, with decay rate constants that are virtually identical for both radical species as shown in Figure 2b,c. This suggests that, not unexpected, an intramolecular BET from $C_{60}^{\bullet-}$ to $ZnP^{\bullet+}$ governs the fate of the **ZnP$^{\bullet+}$-C$_{60}^{\bullet-}$** radical ion pair. In the presence of O_2, the decay rate of both $C_{60}^{\bullet-}$ and $ZnP^{\bullet+}$ absorption is markedly accelerated as compared to that found in the absence of O_2 (Figure 2b,c). Interestingly, the decay rate of $C_{60}^{\bullet-}$ coincides with that of $ZnP^{\bullet+}$ and, in addition, increases linearly with increasing O_2 concentration.[15] The rate constants (k_{BET}) in the absence and presence of O_2 for a series of ZnP-C_{60} linked systems in PhCN are summarized in Table 1.

In contrast to the **ZnP-C$_{60}$** dyad, the k_{BET} from $C_{60}^{\bullet-}$ to ferricenium ion (Fc^+) in **Fc$^+$-ZnP-C$_{60}^{\bullet-}$** under O_2-saturated conditions matches surprisingly the value determined in the absence of O_2 as shown in Figures 3 and 4. It is worth

(11) Bruinink, J.; Kregting, C. G. A.; Ponjee, J. J. *J. Electrochem. Soc.* **1977**, *124*, 1854.

(12) Some porphyrin-C_{60} linked systems produce the charge-separated state even in nonpolar solvents, see for examples: (a) Schuster, D. I.; Cheng, P.; Wilson, S. R.; Prokhorenko, V.; Katterle, M.; Holzwarth, A. R.; Braslavsky, S. E.; Klihm, G.; Williams, R. M.; Luo, C. *J. Am. Chem. Soc.* **1999**, *121*, 11599. (b) Imahori, H.; Hagiwara, K.; Aoki, M.; Akiyama, T.; Taniguchi, S.; Okada, T.; Shirakawa, M.; Sakata, Y. *J. Am. Chem. Soc.* **1996**, *118*, 11771. (c) Guldi, D. M.; Luo, C.; Prato, M.; Dietel, E.; Hirsch, A. *Chem. Commun.* **2000**, 373. (d) Kuciauskas, D.; Liddell, P. A.; Lin, S.; Stone, S. G.; Moore, A. L.; Moore, T. A.; Gust, D. *J. Phys. Chem. B* **2000**, *104*, 4307.

(13) In Figure 2a, the spectrum at 0.1 μs shows small maxima also at 700 and 840 nm, which decayed quickly in 1.0 μs. These minor absorption bands are assigned to the triplet states of C_{60} and ZnP moieties, respectively,[8b] and disappear in the presence of O_2.

(14) (a) Kadish, K. M.; Gao, X.; Van Caemelbecke, E.; Suenobu, T.; Fukuzumi, S. *J. Phys. Chem. A* **2000**, *104*, 3878. (b) Guldi, D. M.; Asmus, K.-D. *J. Phys. Chem. A* **1997**, *101*, 1472.

(15) The O_2 concentrations in air- and O_2-saturated PhCN solutions were determined by the spectroscopic titration for the photooxidation of 10-methyl-9,10-dihydroacridine by O_2, see: Fukuzumi, S.; Ishikawa, M.; Tanaka, T. *J. Chem. Soc., Perkin Trans. 2* **1989**, 1037.

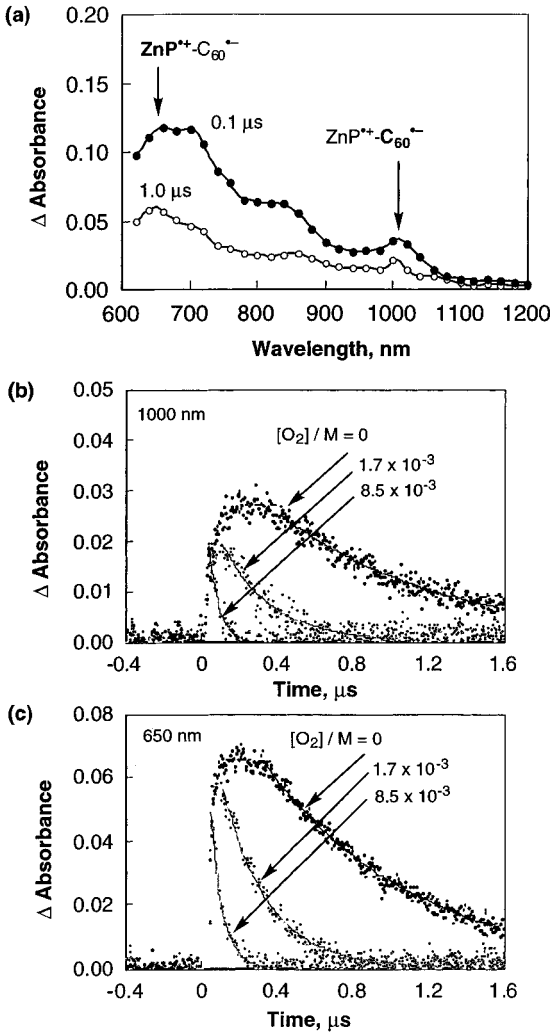

Figure 2. (a) Transient absorption spectra following laser excitation of **ZnP-C$_{60}$** (0.10 and 1.0 μs after the laser pulse) in deoxygenated PhCN. (b) Time profiles of the absorbance at 1000 nm due to $C_{60}^{\bullet-}$ in **ZnP$^{\bullet+}$-C$_{60}^{\bullet-}$**. (c) Time profiles of the absorbance at 650 nm due to $ZnP^{\bullet+}$ in **ZnP$^{\bullet+}$-C$_{60}^{\bullet-}$**. The solid lines show the simulation curves for the first-order decay to give the k_{BET} values in Table 1.

Table 1. Rate Constants k_{BET} for Back Electron Transfer and the Free Energy Change ($-\Delta G^0_{BET}$)[a] in Fullerene-Based Dyad and Triads in the Absence and Presence of O_2 in PhCN

compd	$-\Delta G^0_{BET}$ (eV)	k_{BET} (s^{-1}) at $[O_2]^b$ = 0 M	1.7×10^{-3} M	8.5×10^{-3} M
$ZnP^{\bullet+}$-$C_{60}^{\bullet-}$	1.38	1.3×10^6	3.8×10^6	1.5×10^7
$ZnP^{\bullet+}$-H_2P-$C_{60}^{\bullet-}$	1.34	4.8×10^4	1.1×10^5 (1.2×10^5)[c]	3.2×10^5
Fc^+-ZnP-$C_{60}^{\bullet-}$	1.03	1.3×10^5	1.3×10^5	1.3×10^5

[a] The $-\Delta G^0_{BET}$ values are obtained from the difference between the one-electron oxidation and reduction potentials which are determined by differential pulse voltammetry in PhCN containing 0.1 M Bu_4NPF_6. [b] The O_2 concentrations in air- and O_2-saturated PhCN were determined by the method described in ref 15. [c] $[O_2] = 2.6 \times 10^{-3}$ M.

mentioning that the k_{BET} value in the **Fc-ZnP-C$_{60}$** triad is much smaller than that of the corresponding **ZnP-C$_{60}$** dyad (Table 1), allowing, in principle, a rather large time window for O_2 to react with the photolytically generated radical pair. In general, the smaller k_{BET} value of the triad (**Fc-ZnP-C$_{60}$**: 1.3×10^5 s^{-1}) as compared to that of the dyad (**ZnP-C$_{60}$**: 1.3×10^6 s^{-1}) stems from the larger edge-to-edge distance of the former (R_{ee} = 30.3 Å)[9] relative to the latter (R_{ee} = 11.9 Å).[7,8]

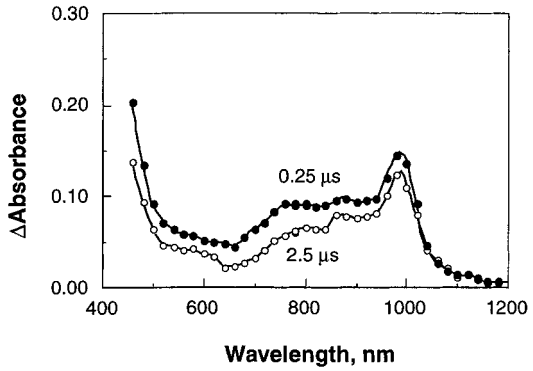

Figure 3. Transient absorption spectra for **Fc-ZnP-C$_{60}$** after laser excitation (0.25 and 2.5 μs after the laser pulse) in deaerated PhCN.

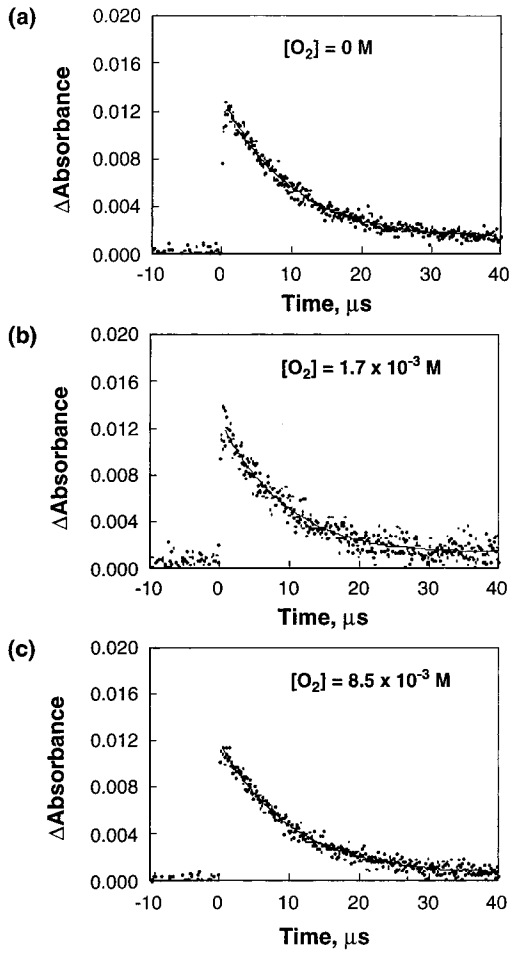

Figure 4. Time profiles of the absorbance at 1000 nm due to $C_{60}^{\bullet-}$ in **Fc$^+$-ZnP-C$_{60}^{\bullet-}$**: (a) in deaerated PhCN, (b) in air-saturated PhCN, and (c) in O_2-saturated PhCN.

Although an even smaller k_{BET} value (4.8×10^4 s^{-1}) was noted for the BET dynamics from $C_{60}^{\bullet-}$ to $ZnP^{\bullet+}$ in the **ZnP$^{\bullet+}$-H$_2$P-C$_{60}^{\bullet-}$** triad, the k_{BET} value is, nevertheless, expedited with increasing O_2 concentration as shown in Table 1. Thus, the presence of $ZnP^{\bullet+}$ appears, without any doubts, essential for the accelerating effect of O_2 on the decay of the radical ion pair.

If the triplet excited state $^3C_{60}$* is energetically close to the radical ion pair state and therefore they are in equilibrium, the apparent lifetime of the radical ion pair may be reduced by the presence of O_2 due to the efficient energy transfer from $^3C_{60}$* to O_2.[16] In the present case, however, the energy level of $^3C_{60}$* in **ZnP-^{3}C$_{60}$*** (1.50 eV) is higher than that of the radical ion

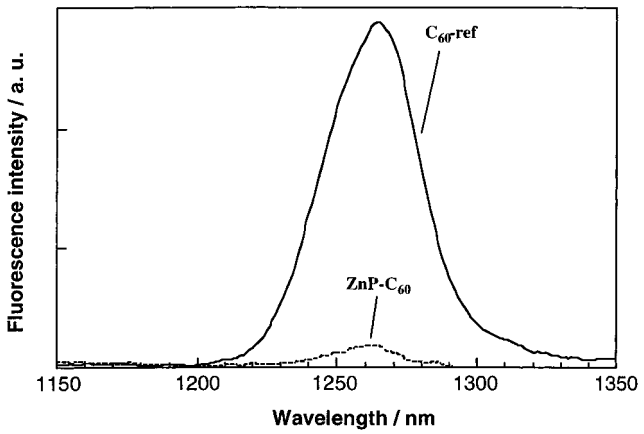

Figure 5. Emission spectra of $^1O_2$ generated from irradiation (λ_{max} = 462 nm) of **C_{60}-ref** (solid line, 1.2×10^{-4} M) and **ZnP-C_{60}** (dotted line, 1.2×10^{-4} M) in oxygen-saturated CD_2Cl_2 under the same experimental conditions.

pair **ZnP$^{\bullet+}$-$C_{60}^{\bullet-}$** (1.38 eV).[8b] In such a case, the concentration of **ZnP-$^3C_{60}$*** is less than 1% as compared to that of **ZnP$^{\bullet+}$-$C_{60}^{\bullet-}$**.[17] Since the rate constant of energy transfer (k_{EN}) from $^3C_{60}$* to O_2 is known to be 1.6×10^9 M^{-1} s^{-1},[18] the decay rate constant of **ZnP$^{\bullet+}$-$C_{60}^{\bullet-}$** via energy transfer from **ZnP-$^3C_{60}$*** to O_2 would be less than 1% of the k_{EN} value. The experimental value is determined as 1.8×10^9 M^{-1} s^{-1} from the slope of the linear correlation between k_{BET} vs [O_2] in Table 1, which is much larger than the expected value for the energy transfer pathway. Thus, it is highly unlikely that the apparent acceleration of the back electron transfer from $C_{60}^{\bullet-}$ to ZnP$^{\bullet+}$ in **ZnP$^{\bullet+}$-$C_{60}^{\bullet-}$** by the presence of O_2 results from the energy transfer from **ZnP$^{\bullet+}$-$C_{60}^{\bullet-}$** to O_2 via the equilibrated **ZnP-$^3C_{60}$***. In fact, the slow rise of the absorbance at 1000 and 650 nm following the initial fast rise (<10 ns) in the absence of O_2 observed in Figure 2a,b is ascribed to the electron transfer from ZnP to $^3C_{60}$* in **ZnP-$^3C_{60}$*** to produce **ZnP$^{\bullet+}$-$C_{60}^{\bullet-}$**. This is consistent with the fact that the energy level **ZnP$^{\bullet+}$-$C_{60}^{\bullet-}$** is lower than that of **ZnP-$^3C_{60}$*** (vide supra). The initial fast rise corresponds to formation of **ZnP$^{\bullet+}$-$C_{60}^{\bullet-}$** via ^{1}ZnP* and $^1C_{60}$*, which is the major part as compared to the formation via $^3C_{60}$*. In any case, an energy transfer from $^3C_{60}$* to O_2 should result in formation of singlet oxygen ($^1\Delta_g$).[19] A quantitative singlet oxygen generation is well-known for fullerenes[20] and, in fact, irradiation of **C_{60}-ref** (1.2×10^{-4} M) led to the characteristic $^1\Delta_g$ O_2 phosphorescence at 1270 nm with $\Phi \sim 1$ (see Figure 5). In contrast, the intensity of $^1\Delta_g$ O_2 phosphorescence was significantly reduced as compared to **C_{60}-ref** upon irradiating **ZnP-C_{60}** dyad under identical conditions (Figure 5). This indicates that the energy transfer pathway from **ZnP$^{\bullet+}$-$C_{60}^{\bullet-}$** via **ZnP-$^3C_{60}$*** can be ruled out as a major contributor to the decay of the radical ion pair, with high certainty as shown in Scheme 1. The observation of much smaller intensity of $^1\Delta_g$ O_2 phosphorescence of the **ZnP-C_{60}** system as compared to **C_{60}-ref** may well be ascribed to the energy transfer from $^3C_{60}$* in **ZnP-$^3C_{60}$***, the concentration of which is much smaller than that of **ZnP$^{\bullet+}$-$C_{60}^{\bullet-}$**, to O_2, in competition with electron transfer from ZnP to $^3C_{60}$* (Scheme 1).

Scheme 1

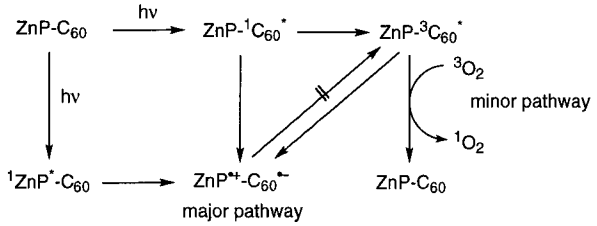

In an aqueous solution an electron transfer from $C_{60}^{\bullet-}$ to O_2 has been reported to occur, although the direct detection of $O_2^{\bullet-}$ produced in the electron transfer has yet to be confirmed.[21,22] Oxygen is known to be reduced much easier in water as compared to the reduction in an aprotic solvent due to the effect of the stronger solvation of $O_2^{\bullet-}$ in water as confirmed by the large shift of -0.44 V for the $O_2/O_2^{\bullet-}$ couple on going from water to an aprotic solvent (diemthylformamide).[23] To determine the energetics of electron transfer from $C_{60}^{\bullet-}$ to O_2 accurately, the one-electron reduction potentials of **C_{60}-ref** and O_2 were determined in benzonitrile under the same experimental conditions using the ferrocene/ferricenium (Fc/Fc^+) reference (see Experimental Section). The electron transfer from $C_{60}^{\bullet-}$ to O_2 is found to be endergonic [$\Delta G^0_{et} \gg 0$ (0.28 eV)], judging from the one-electron reduction potentials of both species: E^0_{red} of O_2 (-1.33 V vs Fc/Fc^+)[24−26] is significantly lower than that of **C_{60}-ref** (-1.05 V vs Fc/Fc^+). Thus, a direct electron transfer from $C_{60}^{\bullet-}$ in **ZnP$^{\bullet+}$-$C_{60}^{\bullet-}$** to O_2 is highly unlikely to occur in benzonitrile. In addition, the concomitant decay of ZnP$^{\bullet+}$ and $C_{60}^{\bullet-}$ in Figure 2 is inconsistent with a direct electron transfer from $C_{60}^{\bullet-}$ to O_2, which would yield stable **ZnP$^{\bullet+}$-C_{60}** and $O_2^{\bullet-}$ on the present time scale. To further test this hypothesis, the much better electron acceptor, hexyl viologen (HV^{2+}) (-0.79 V vs Fc/Fc^+), was probed as an O_2 surrogate. Indeed, a direct electron transfer from $C_{60}^{\bullet-}$ to HV^{2+} occurs, producing $HV^{\bullet+}$. Importantly, the transient features of ZnP$^{\bullet+}$ were not affected by this reaction and remained virtually stable on the monitored time scale as shown in Figure 6.[27] The second-order ET rate constant was determined as 5.0×10^9 M^{-1} s^{-1} from the dependence of the ET rate on the HV^{2+} concentration.

In the presence of metal ions, $O_2^{\bullet-}$ is known to coordinate to the metal ion, yielding the corresponding $O_2^{\bullet-}$−metal ion complex.[28,29] This can, of course, only occur when the one-

(16) (a) Fujitsuka, M.; Ito, O.: Yamashiro, T.; Aso, Y.; Otsubo, T. *J. Phys. Chem. A* **2000**, *104*, 4876. (b) Ito, O.; Yamazaki, M.; Fujitsuka, M. In *Fullerenes 2000-Volume 8, Electrochemistry and Photochemistry*; Fukuzumi, S., D'Souza, F., Guldi, D. M., Eds.; The Electrochemical Soceity: Pennington, 2000; pp 306−318.

(17) The ratio of [**ZnP-$^3C_{60}$***]/[**ZnP$^{\bullet+}$-$C_{60}^{\bullet-}$**] is obtained as $\exp(-0.12/k_BT) = 0.0093$ at 298 K (k_B is the Boltzmann constant).

(18) Guldi, D. M.; Kamat, P. V. *Fullerenes: Chemistry, Physics, and Technology*; Kadish, K. M., Ruoff, R. S., Ed.; Wiley: New York, 2000; Chapter 5, p 225.

(19) *Singlet Oxygen*; Frimer, A. A., Ed.; CRC: Boca Raton, FL, 1985; Vols. I−IV and references therein.

(20) (a) Arbogast, J. W.; Darmanyan, A. P.; Foote, C. S.; Rubin, Y.; Diederich, F. N.; Alvarez, M. M.; Anz, S. J.; Whetten, R. L. *J. Phys. Chem.* **1991**, *95*, 11. (b) Prat, F.; Stackow, R.; Bernstein, R.; Qian, W.; Rubin, Y.; Foote, C. S. *J. Phys. Chem. A* **1999**, *103*, 7230. (c) Da Ros, T.; Prato, M. *Chem. Commun.* **1999**, 663.

(21) Yamakoshi, Y.; Sueyoshi, S.; Fukuhara, K.; Miyata, N.; Masumizu, T.; Kohno, M. *J. Am. Chem. Soc.* **1998**, *120*, 12363.

(22) (a) Imahori, H.; Yamada, H.; Ozawa, S.; Ushida, K.; Sakata, Y. *Chem. Commun.* **1999**, 1165. (b) Imahori, H.; Yamada, H.; Nishimura, Y.; Yamazaki, I.; Sakata, Y. *J. Phys. Chem. B*, **2000**, *104*, 2099.

(23) Sawyer, D. T.; Valentine, J. S. *Acc. Chem. Res.* **1981**, *14*, 393.

(24) It has been confirmed that $E_{1/2}$ of O_2 is the same irrespective of the different sweep rate of the cyclic votammogram.

(25) A slightly less negative E^0_{red} value of O_2 (-0.86 V vs SCE = -1.23 V vs Fc/Fc^+) has been reported in acetonitrile: Sawyer, D. T.; Calderwood, T. S.; Yamaguchi, K.; Angelis, C. T. *Inorg. Chem.* **1983**, *22*, 2577.

(26) The E^0_{red} value of O_2 reported in ref 8b has to be corrected to the value in benzonitirile.

(27) The intermolecular back electron transfer from $HV^{\bullet+}$ to **ZnP$^{\bullet+}$-C_{60}** is negligible on the present time scale due to the low concentration.

(28) Fukuzumi, S.; Patz, M.; Suenobu, T.; Kuwahara, Y.; Itoh, S. *J. Am. Chem. Soc.* **1999**, *121*, 1605.

(29) Fukuzumi, S.; Ohkubo, K. *Chem. Eur. J.* **2000**, *6*, 4532.

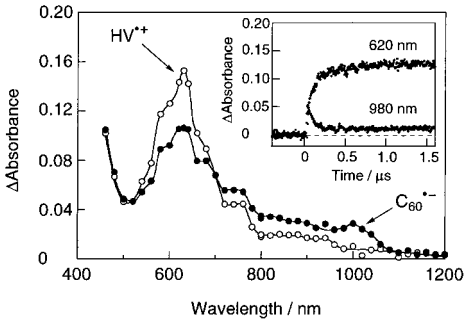

Figure 6. Transient absorption spectra of a PhCN solution containing **Fc-ZnP-C$_{60}$** (0.1 mM) and HV^{2+} (5.0 mM) after laser excitation (100 ns and 1 μs) in deaerated PhCN. Inset: Absorption−time profiles at 620 and 980 nm.

electron reduction potential of O_2 is shifted to positive directions.[5,6] In the case of **ZnP$^{\bullet+}$-C$_{60}^{\bullet-}$** and **ZnP$^{\bullet+}$-H$_2$P-C$_{60}^{\bullet-}$**, $O_2^{\bullet-}$ can coordinate to ZnP$^{\bullet+}$, when an intermolecular reaction between $C_{60}^{\bullet-}$ and O_2 renders it energetically feasible.[30] The binding energies of $O_2^{\bullet-}$ with various divalent metal ions (Mg^{2+}, Ca^{2+}, Sr^{2+}, and Ba^{2+}) have recently been determined as 0.5−0.7 eV,[29,31] which is sufficient to make an electron transfer from $C_{60}^{\bullet-}$ to O_2 energetically feasible. In contrast to the ZnP-containing donor−acceptor systems, ferrocene is a fully coordinated complex, omitting the coordination of another ligand, such as $O_2^{\bullet-}$. As a matter of fact, this seems the likely rationale for the lack of accelerating effects in the **Fc^{+}-ZnP-C$_{60}^{\bullet-}$** system.

The catalytic participation of O_2 in an intramolecular BET between $C_{60}^{\bullet-}$ and ZnP$^{\bullet+}$ in ZnP-linked C_{60} is depicted in Scheme 2.[32] The intermolecular ET from $C_{60}^{\bullet-}$ to O_2 may be initiated by the coordination of O_2 to ZnP$^{\bullet+}$, followed by electron transfer from $C_{60}^{\bullet-}$ to O_2 coordinated to ZnP$^{\bullet+}$ to yield $O_2^{\bullet-}$ bound to ZnP$^{\bullet+}$. Due to the strong binding of $O_2^{\bullet-}$ to ZnP$^{\bullet+}$, the one-electron reduction potential of O_2 is shifted toward positive values, namely, in favor of the ET event.[30,31] The complexation is then followed by a rapid intramolecular ET from $O_2^{\bullet-}$ to ZnP$^{\bullet+}$ in the $O_2^{\bullet-}$-ZnP$^{\bullet+}$ complex to regenerate O_2 (Scheme 2a). By applying the steady-state approximation to the intermediates in Scheme 2, the observed back electron-transfer rate constant k_{BET} is given by eq 1.[32]

$$k_{BET} = k_{ET}k_1[O_2]/(k_{-1} + k_{ET}) \quad (1)$$

The second-order rate constant $[k_{ET}k_1/(k_{-1} + k_{ET})]$ of **ZnP$^{\bullet+}$-C$_{60}^{\bullet-}$** (1.6×10^9 M^{-1} s^{-1}) obtained from the linear dependence of k_{BET} on $[O_2]$ in PhCN is only slightly lower than the diffusion-controlled limit in PhCN (5.6×10^9 M^{-1} s^{-1}). Such a fast rate is inconsistent with the back electron transfer via the energy

Scheme 2

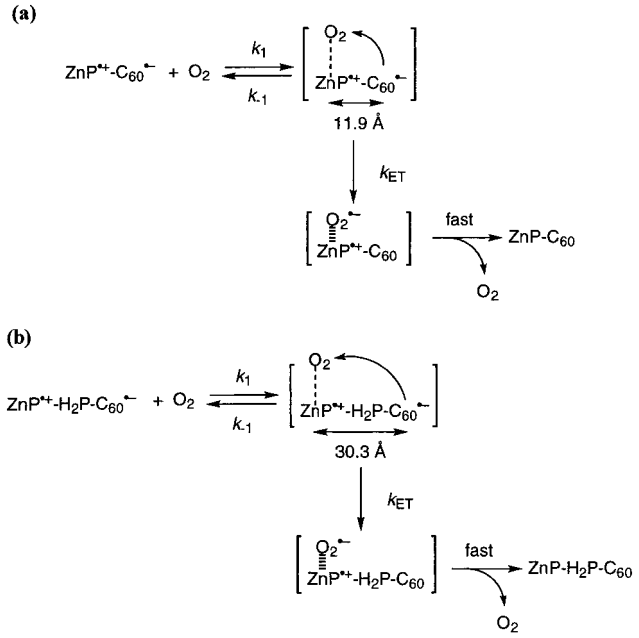

transfer from the high-lying triplet excited state ($^3C_{60}$*) to O_2 (vide infra) as already indicated by the $^1\Delta_g$ O_2 phosphorescence measurements (Figure 5). On the other hand, the corresponding value of **ZnP$^{\bullet+}$-H$_2$P-C$_{60}^{\bullet-}$** (3.3×10^7 M^{-1} s^{-1}) is 48 times smaller as compared to the value of **ZnP$^{\bullet+}$-C$_{60}^{\bullet-}$**. Such a decreased rate for **ZnP$^{\bullet+}$-H$_2$P-C$_{60}^{\bullet-}$** as compared to **ZnP$^{\bullet+}$-C$_{60}^{\bullet-}$** is also inconsistent with the energy transfer pathway, since the triplet energy of $^3C_{60}$* is essentially the same between **ZnP-^{3}C$_{60}$*** and **ZnP-H$_2$P-^{3}C$_{60}$***. Remarkably, this k_{ET} ratio (48) is consistent with the k_{BET} ratio (27) (i.e., from $C_{60}^{\bullet-}$ to ZnP$^{\bullet+}$) between the triad and the dyad, however, in the absence of O_2. Thus, ET from **ZnP$^{\bullet+}$-H$_2$P-C$_{60}^{\bullet-}$** to O_2 occurs even at the longer distance as compared to ET from the **ZnP$^{\bullet+}$-C$_{60}^{\bullet-}$** dyad, since O_2 is placed at a longer distance from $C_{60}^{\bullet-}$ in the precursor complex for the electron transfer from $C_{60}^{\bullet-}$ to O_2 in **ZnP$^{\bullet+}$-H$_2$P-C$_{60}^{\bullet-}$** (see Scheme 2b as compared to Scheme 2a). This is in sharp contrast to the truly intermolecular ET from **ZnP$^{\bullet+}$-H$_2$P-C$_{60}^{\bullet-}$** and **ZnP$^{\bullet+}$-C$_{60}^{\bullet-}$** to HV^{2+}, which occur with nearly diffusion-controlled rates.

In conclusion, O_2 acts as a novel *catalyst* to expedite intramolecular BET in ZnP-linked C_{60} systems where ZnP$^{\bullet+}$ accelerates the reaction of $C_{60}^{\bullet-}$ with O_2 and, in turn, activates the catalysis of O_2 in the overall BET from $C_{60}^{\bullet-}$ to ZnP$^{\bullet+}$ (Scheme 2).

Acknowledgment. We are grateful to Mr. S. Fujita for his help in measuring the $^1\Delta_g$ O_2 phosphorescence spectrum. This work was supported by a Grant-in-Aid for Scientific Research Priority Area (No. 11228205) from the Ministry of Education, Science, Sports and Culture, Japan, the Sumitomo Foundation, and the Office of Basic Energy Sciences of the Department of Energy (document NDRL-4264 from the Notre Dame Radiation Laboratory).

JA002052U

(30) The one-electron reduction potential of O_2 in the presence of 0.10 M $HClO_4$ in MeCN has been reported to be shifted from −0.86 V (vs SCE) to −0.21 V (vs SCE); see: Fukuzumi, S.; Mochizuki, S.; Tanaka, T. *Inorg. Chem.* **1989**, *28*, 2459. The potential shift in the presence of ZnP$^{\bullet+}$ which can act as a hard acid may also be positive enough to make the ET from $C_{60}^{\bullet-}$ to O_2 energetically feasible.

(31) The strong coordination of $O_2^{\bullet-}$ to Zn(II) ion has also been indicated; see: Ohtsu, H.; Shimazaki, Y.; Odani, A.; Yamauchi, O.; Mori, W.; Itoh, S.; Fukuzumi, S. *J. Am. Chem. Soc.* **2000**, *122*, 5733.

(32) We appreciate very much the reviewer's suggestion about Scheme 2 and eq 1.